# Asymmetric Response in a Line of Optically Driven Metallic Nanospheres

**J. V. Hernández*,† L. D. Noordam,‡ and F. Robicheaux†**

*Department of Physics, Auburn University, Auburn, Alabama 36849, and FOM Institute for Atomic and Molecular Physics, Kruislaan 407, 1098 SJ Amsterdam, The Netherlands*

*Received: May 24, 2005; In Final Form: June 29, 2005*

We describe the dipole−dipole interactions between a linear array of optically driven silver metallic nanospheres (MNSs). These model calculations incorporate the full electric field generated by an oscillating dipole and predict several interesting effects due to the retardation of the field. The distribution of the power associated with MNSs along the array shows a strong variation on a scale smaller than the wavelength of the driving light. For a given geometry, there is a small range of frequencies where the relative power in the last MNS compared to the first dramatically changes, suggesting a simple device for wavelength discrimination in this frequency range. Moreover, small changes in the driving frequency can completely change the direction of the scattered light when only a single nanosphere is driven.

## 1. Introduction and Summary

Recently there have been many theoretical and experimental studies probing the nature of a collection of optically driven metal nanospheres (MNSs), their interactions, and various possible uses as subwavelength optical devices.[1−13] Arrangements of MNSs with features smaller than the wavelength of light, $\lambda$, can be constructed and will interact strongly with light tuned to the surface plasmon (SP) frequency ($\omega_{SP}$).[14] The coupling of the MNSs through the electromagnetic field produces a coherent wave of oscillating dipole moments. This coupling allows information to pass through geometries smaller than $\lambda$ and causes the direction of the scattered light to strongly depend on $\lambda$. A simple and important geometry to study is a straight line or chain of equally spaced MNSs placed in a dielectric medium. This configuration is shown in Figure 1 with a realistic particle size and spacing. In this paper we will use an array of 10 nanospheres; it has been shown when using common parameters that the infinite chain limit is met at around 10 particles.[11] A technique for the fabrication of such assemblies is electron-beam lithography, which allows for good control over particle size and regular placement.[7] Being one of the easiest configurations to set up experimentally and theoretically, it has been studied extensively. All of the MNSs in the linear array can be excited using a broad light beam at a specific frequency $\omega$. Theoretical analysis of a linear array of MNSs has been done by several different groups. The numerical methods developed to describe these arrays and their interactions with an external electric field include the discrete dipole approximation,[8] the multiple multipole method,[10] the finite difference time domain method,[7] and the T-matrix method.[2] The method used in this paper can perhaps best be described as the coupled dipole approximation. Each nanosphere will be described by a single point dipole that linearly responds to electric fields. When the system is driven at a specific frequency, $\omega$, then every time-dependent quantity can be written as $A(t) = A(0)\exp(-i\omega t)$. We will solve a set of self-consistent linear equations describing the response of each electric dipole to the incident field and to the scattered electric fields from the other particles. In doing so, we will use the full electric field from the oscillating dipoles and contrast these results with using only the near-field approximation. We report several interesting effects apparent in this simple system that emerge from treating the full field rather than the near field. We show that the ohmic power deposited in a particular MNS can strongly depend on the position in the line of particles even when all of the MNS are equally illuminated by a light beam. Furthermore, we can reverse the ratio of power in the first sphere compared to the last sphere with an extremely small variation in light frequency, suggesting a device for wavelength discrimination over this range of frequencies. Also, we will show that the direction of the light emitted from the MNS array strongly depends on frequency when only one of the spheres is driven. Thus, it should be possible to detect collective properties of the MNS array, such as inhomogeneous power distribution along the array, using simple measurements of the far-field radiation, which could simplify experiments.

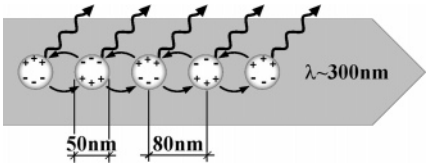


**Figure 1.** Schematic drawing of a possible setup for a regularly spaced linear array of silver nanospheres. A wide (compared to the size of a nanosphere of radius *a*) beam of light of frequency $\omega$ is propagated along the array's axis in the particular medium where the array is assembled. The light absorbed and scattered by each MNS will in turn excite neighboring MNSs, and a coherent wave of oscillating electric dipoles will be produced.

There are three uncoupled modes of propagation down this chain: two (degenerate) transverse (T) waves having the direction of the dipole moments, $\vec{p}$, perpendicular to the line of MNSs and a longitudinal (L) mode in which $\vec{p}$ are parallel to the chain axis. All other forms of propagation can be described as a linear combination of T and L modes. For the T modes, widely separated MNSs can interact via the far field of the scattered light, while this is not possible for the L modes since there is no scattered light parallel to the dipole moment. A very

* To whom correspondence should be addressed.
† Auburn University.
‡ FOM Institute for Atomic and Molecular Physics.

10.1021/jp0527352 CCC: $30.25 
Published on Web 08/04/2005

thorough study on the effect of the far field of the scattered light on the dispersion relation of T modes was done by Citrin.[12] For the geometry discussed in this paper, the light beam will be directed from left to right, and thus, only T modes are excited unless noted otherwise.

## 2. Method

In our calculations, we assume that the plasmon excitations caused by incident light produce an oscillating dipole electric field. This assumption holds if the wavelength of the incident light is much larger than the diameter, $2a$, of the MNS and the interparticle distance $d \gtrsim 3a$.[10,15] A more complete investigation of higher order multipole effects in the near field has been done in ref 10; higher order multipole effects become increasingly important as the interparticle spacing decreases but should give only minor, quantitative differences for the cases we present here. The electric field produced by a single, periodically oscillating dipole with an electric dipole moment $\vec{p}$ is given by

$$\vec{E}(\vec{p},\vec{R},k) = \frac{1}{4\pi\epsilon}\left\{k^2(\hat{R}\times\vec{p})\times\hat{R}\,\frac{e^{ikR}}{R} + [3\hat{R}(\hat{R}\cdot\vec{p}) - \vec{p}]\left(\frac{1}{R^3} - \frac{ik}{R^2}\right)e^{ikR}\right\} \quad (1)$$

where $k = \omega/v$ is the wavenumber in the dielectric, $v$ is the speed of light in the dielectric medium,[16] and $\hat{R}$ is the unit vector in the direction of $\vec{R}$ ($\vec{R}$ is the displacement from the dipole $\vec{p}$).[15] If we use the near-field approximation, $R \ll \lambda$, then we set $k = 0$ and the electric field is

$$\vec{E}_{\text{near}}(\vec{p},\vec{R}) = -\frac{1}{4\pi\epsilon}\frac{\vec{p} - 3\hat{R}(\vec{p}\cdot\hat{R})}{R^3} \quad (2)$$

In the near field the electric field is dominant, but when using the full field this is not immediately obvious. We can neglect the effects of the magnetic field, however, if the charge separation is small, i.e., the magnitude of the dipole is not very large compared to the total charge times the radius $a$ on the MNS. Using the full electric dipole fields we can construct self-consistent equations of motion for a driven system of MNSs. The equation of motion for a dipole driven by an electric field can be parametrized as $\ddot{\vec{p}} + \gamma\dot{\vec{p}} + \omega_{\text{SP}}^2\vec{p} - \beta\dddot{\vec{p}} = \eta\vec{E}(t)$ where $\gamma$, $\omega_{\text{SP}}$, $\beta$, and $\eta$ are constants; the physical values of these parameters are substituted in the equation below. The terms of this equation have a familiar origin: the first term is the acceleration, the second term is the damping from ohmic heating, the third term is from the harmonic force, the fourth term is from radiation damping, and the right-hand side is the driving term from the electric field. Substituting the oscillating form, $\vec{p}_n(t) = \vec{p}_n\exp(-i\omega t)$, and substituting the physical values for the constants gives the coupled dipole−dipole equations of motion:

$$\left[-\omega^2 - i\gamma\omega + {\omega_{\text{SP}}}^2 - i\frac{2}{9}\left(\frac{a}{v}\right)^3{\omega_{\text{p}}}^2\omega^3\right]\vec{p}_n = \frac{1}{3}a^3{\omega_{\text{p}}}^2 4\pi\epsilon\{\vec{E}_n^{(\text{ext})} + \sum_{n'\neq n}\vec{E}(\vec{p}_{n'},\vec{R}_{nn'},k)\} \quad (3)$$

where $a$ is the radius of the MNS, $\vec{R}_{nn'} \equiv \vec{R}_{n'} - \vec{R}_n$ is the center-to-center distance between two particles, $\vec{E}_n^{(\text{ext})}$ is the external electric field at the $n$th nanosphere, and $\vec{E}(\vec{p}_{n'},\vec{R}_{nn'},k)$ has been defined in eq 2. In a previous study, the radiation damping was erroneously taken to be negligibly small.[6] For the parameters of this paper, the radiation damping is the largest loss mechanism, but the radiation damping does become less important as the radius of the MNSs decreases. In the ohmic damping term, $\gamma$ is the inverse of the electronic relaxation time. To match the bulk dielectric properties of Ag, we use a value of $\gamma = 7.87 \times 10^{13}$ s$^{-1}$.[6] The coupling strength is determined in large part by the bulk plasmon frequency $\omega_{\text{p}}$. The value of $\omega_{\text{p}}$ has been defined such that ${\omega_{\text{p}}}^2 = (Ne^2)/(\epsilon m^*)$, where $N$ is the total number of conducting electrons per unit volume, $e$ is the charge of an electron, and $m^*$ is the optical effective electron mass.[17] For silver we used $N = 5.85 \times 10^{28}$ electrons/m$^3$ and $m^* = 8.7 \times 10^{-31}$kg. We have calculated a value of $\omega_{\text{p}} \approx 9.3 \times 10^{15}$ rad/s, and we will use $\omega_{\text{SP}} \approx 5 \times 10^{15}$ rad/s.[6] The solutions to these coupled inhomogeneous linear algebra equations are the induced dipole moments, $\vec{p}$, on each sphere. Because $\vec{p}$ appears linearly, these coupled equations can be solved directly by using standard linear algebra packages.

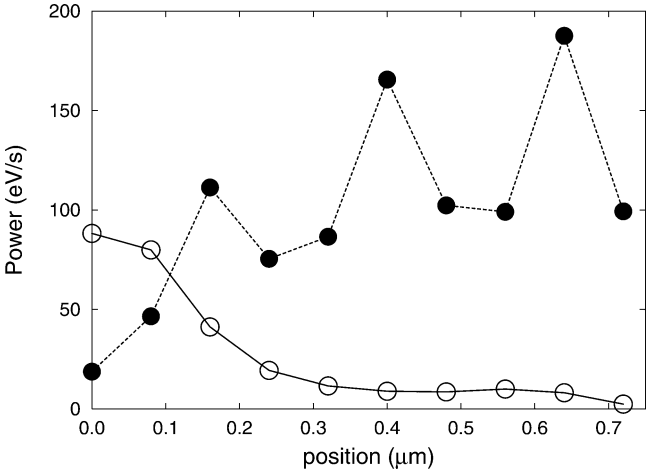


**Figure 2.** Ohmic power as a function of the position of 10 MNSs in a regularly spaced linear array. The center-to-center interparticle distance is $d = 80$ nm, and the diameter, $2a$, of each MNS is 50 nm. A plane transversely polarized electromagnetic wave is propagated from left to right along the axis of the array. All of the MNSs absorb and scatter the incident electromagnetic wave of magnitude 1 V/m. The solid line is for a chosen frequency $\omega = 4.85 \times 10^{15}$ rad/s ($\lambda_{\text{diel}} = 259$ nm) when most of the power is in the first sphere. The dashed line is for a frequency of $\omega = 4.62 \times 10^{15}$ rad/s ($\lambda_{\text{diel}} = 272$ nm) when most of the power is in the last sphere. This asymmetry between first and last MNSs vanishes in the near-field approximation at all wavelengths.

## 3. Results

The MNSs act as both scatterers and detectors of the total electromagnetic field. The induced dipole moment of an MNS is proportional to the local electric field, while the ohmic power dumped into the MNS is proportional to the magnitude of the dipole moment squared. In Figure 2 the ohmic power of each of the 10 individual MNSs is plotted for two specific frequencies: one placing most of the power on the first MNS and the other directing most of the power down the chain. In both cases the magnitude of the incident electric field is chosen to be 1 V/m to facilitate (through linear scaling) the calculation of the power at other field strengths. The dramatic difference in the distribution of power with relatively small changes in frequency is evident. The near-field approximation has been used in many studies of interacting MNSs, but does not correctly reproduce most effects in Figure 2. The near-field approximation is most accurate when $kd \ll 1$, $d$ being the regular center-to-center interparticle distance. In the case of Ag nanospheres $\omega_{\text{SP}} \approx 5 \times 10^{15}$ rad/s, which gives a value of $k \approx 3.0 \times 10^7$ m$^{-1}$, in

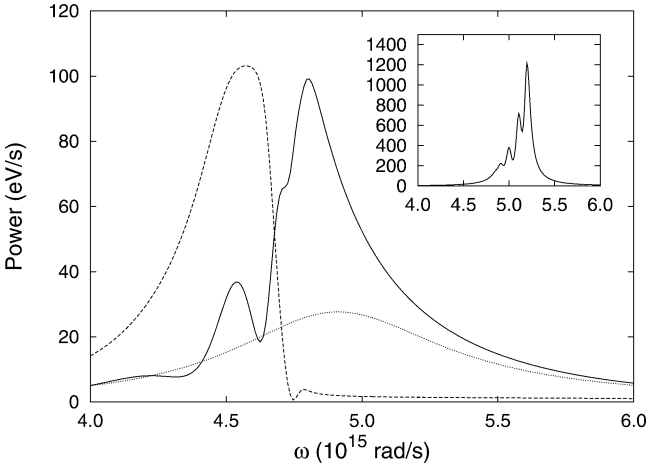


**Figure 3.** Ohmic power as a function of the frequency, $\omega$, of a plane electromagnetic wave propagating along the axis of a regular linear array of MNSs. The dimension of the array and MNSs is the same as in Figures 1 and 2. All of the MNSs absorb and scatter the incident beam of light as it comes in from left to right. The solid line is the ohmic power of the first (leftmost) MNS, and the dashed line is for the last (10th) one. The dotted line is the power response for the single MNS case. The inset is the same as the main figure, but using only the near-field approximation. Note that it is now impossible to preferentially excite the first or last MNS by modifying the driving frequency.

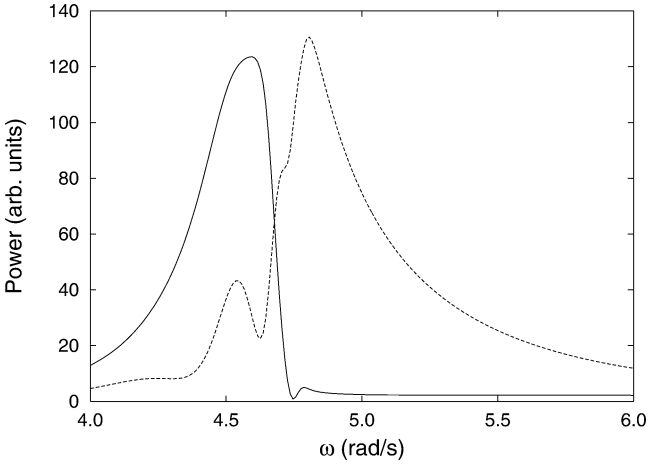


**Figure 4.** Same physical set up as Figure 2, but this time only the first sphere is externally excited. Plotted is the differential radiated power per solid angle versus the frequency of the incident light. The solid line is the power scattered in the forward direction, and the dashed line is the power scattered in the backward direction.

the dielectric. Typical interparticle spacings are in the range of 80 nm, so in these cases $kd \approx 2\pi/3$. In the near-field approximation, coupling terms that fall off as $R^{-1}$ and $R^{-2}$ are neglected. When using the full electric field, certain phase-dependent phenomena are now taken into account that had been overlooked in earlier work.[6] It is important to recognize that the dipole fields created by the now oscillating electric dipoles have individual phases that vary with the distance from an MNS. The retarded electric field can add either constructively or destructively down the chain to create localized regions of high total electric field. Using the near-field approximation, all of the MNSs "talk" to each other instantaneously, and any phase is solely due to the phase of oscillation of a single dipole. Using this approximation, the ohmic power is symmetric through the midpoint of the array at all wavelengths. In contrast, when using the full dipole field, there is a lag in interparticle communication due to the finite speed of light. It is this lag that allows the MNSs to have differing phases that can coherently add or subtract at specific locations in space.

It is also interesting to compare the ohmic power of the first MNS to the last one while scanning over a range of frequencies. Remember that in our geometry the light is directed down the line of MNSs. Therefore, without the interaction between MNSs, each of the nanospheres would dissipate the same amount of ohmic power. It can immediately be seen in Figure 3 that within a certain band of frequencies the ohmic power from the first sphere is much greater than that of the last one. Within another band of frequencies the opposite is true. A similar though lesser effect is present even for the limit of two MNSs. To clearly illustrate the sensitivity of the array, we also plotted the single particle response to an identical beam of light in Figure 3 as dotted lines. Note that the response of the first MNS follows the response of a single sphere when the driving frequency is far off resonance, but the response of the last sphere is strongly suppressed for all of the plotted frequencies greater than resonance. This forward−backward asymmetry is not present when the near-field approximation is used (inset of Figure 3), and thus the asymmetry is due solely to the retardation of the electric field. It is also interesting that the power in the first sphere is greater than for a single sphere for almost all frequencies and is roughly a factor of 3 times larger at the peak. Naturally the next step is to investigate what is the cause of the forward−backward frequency-dependent asymmetry as seen in Figure 3. Using the calculated dipole moments and looking in the far-field ($r \rightarrow \infty$) limit we can determine the differential radiated power per solid angle:[15]

$$\frac{dP_{rad}}{d\Omega} = \frac{1}{2}\frac{\upsilon k^4}{(4\pi)^2\epsilon}[\,|\vec{p}|^2 - |\,\hat{r}\cdot\vec{p}|^2] \tag{4}$$

where

$$\vec{p} \equiv \sum_n \vec{p}_n\, e^{-ik\hat{r}\cdot\vec{\Delta}_n} \tag{5}$$

and $k = \omega/\upsilon = 2\pi/\lambda$ is the wavenumber in the dielectric medium. In eqs 5 and 6 $\hat{r}$ is the usual radial unit vector and $\vec{\Delta}_n$ is the displacement from the first nanosphere to the $n$th one; $|\vec{\Delta}_n| = (n-1)d$ for a regularly spaced linear array. We set up a regular linear array as in Figure 1, but we changed the simulation so that only the first (leftmost) MNS is excited to a frequency $\omega$. Exciting a single MNS can probably be realized by using an electron beam instead of optical radiation. Optical spot sizes are on at least the order of $\lambda$ in dielectric, while e-beams can have spot sizes much smaller than the interparticle separation $d$. We can see in Figure 4 that there are indeed certain bands of frequency that cause the whole system to scatter light in the backward direction and that these frequencies are the same frequencies where the forward−backward asymmetry is realized. In fact the similarity between Figures 3 and 4 is quite pronounced, showing that the asymmetric behavior is caused by the coherent constructive or destructive interference of the radiated light from the individual MNS. When driving the first MNS at certain frequencies, the total electric field emitted by the MNSs adds constructively along the line, which correlates with a large amplitude at the last sphere. At other frequencies, the total electric field gives destructive interference along the line, which correlates with the small amplitudes at the final sphere. Another way to look at Figure 4 is to perform a discrete Fourier transform of the induced dipole moments: $\vec{p}(k) = \sum_n \vec{p}(\hat{r}\cdot\vec{\Delta}_n)\exp(-ik\hat{r}\cdot\vec{\Delta}_n)$. We examined $p(k)$ at various $\omega$'s by starting from about $4.0 \times 10^{15}$ rad/s and increasing the frequency. At first a clear peak could be seen in $p(k)$, and this

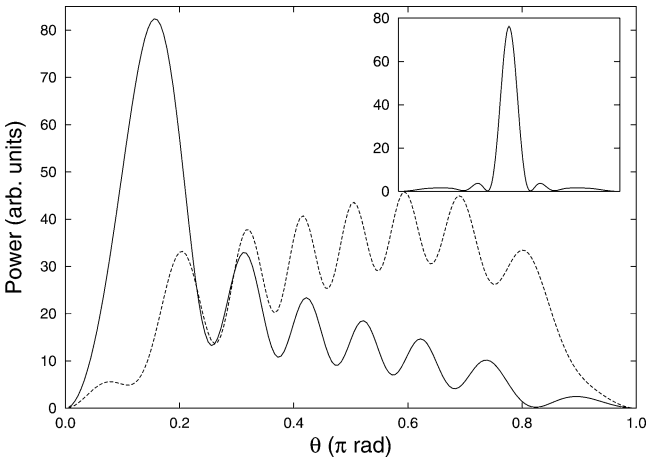


**Figure 5.** Again the same physical setup as Figure 4, but this time the first sphere is externally excited into an L mode. Plotted is the differential radiated power per solid angle versus the scattering angle $\theta$ for two frequencies, where $\theta$ is the angle relative to the line of MNSs. The solid line is the power scattered at $\omega = \omega_{SP} = 5.0 \times 10^{15}$ rad/s, and the dashed line is the power scattered when $\omega = 5.5 \times 10^{15}$ rad/s. To more cleary show the asymmetry, the dashed line is scaled by 2.0, i.e., the amplitude of the driving force is increased by about 40%. The intermediate electric field of the oscillating dipoles gives the asymmetry. The inset also plots differential radiated power per solid angle versus the scattering angle for $\omega = \omega_{SP}$, but here the MNSs are forced to oscillate in phase.

peak increased as we increased $\omega$. At around $\omega \approx 4.8 \times 10^{15}$ rad/s a clear peak could no longer be discerned and $p(k)$ becomes very noisy. This implies that above about $\omega \approx 4.8 \times 10^{15}$ rad/s we are trying to drive the system outside the allowed photonic bands. This behavior matches closely with Figure 4, suggesting that scattering light in the forward direction is suppressed due to driving outside the photonic band gap for this system. It also suggests that a correct band structure calculation must take into account the full electric dipole field and radiative damping. When exciting the system into L modes, widely separated MNSs do not interact via the far field of the scattered light ($\hat{R} \times \vec{p} = 0$). They do still communicate through the near and intermediate fields. Unlike using the near-field approximation however, the scattered field is still retarded. This retardation will once again cause MNSs to oscillate at various phases allowing for interference effects. In Figure 5 we again use the same physical setup as Figure 1, and we excite only the leftmost MNS at a various frequencies $\omega$. This time we excite into an L mode (parallel to the chain). Plotted in Figure 5 is the differential power scattered per solid angle ($dP/d\Omega$) versus the scattering angle $\theta$ at two different frequencies. The inset is also $dP/d\Omega$, but forcing all of the MNSs to oscillate in phase. This plot is reminiscent of the symmetric diffraction pattern of light passing through slits spaced closely relative to the incident wavelength. A clear asymmetry, however, can be seen in the main plot. As seen with the T mode case, the bulk of the scattered light can be preferentially aimed in different directions by adjusting the frequency of the driving force.

## 4. Conclusion

In summary we have shown that when looking at a system of MNSs, interesting effects can be lost when using only a near-field approximation. Within certain closely spaced bands of frequencies it is possible, using a spatially broad beam of light, to excite specific MNSs. In Figure 3, the ratio of the power in the first sphere to that in the last sphere is 1 near the crossing frequency $\sim 4.7 \times 10^{15}$ rad/s; near this frequency, the ratio varies by more than an order of magnitude in a small range of frequencies. Various experimental techniques can detect when the surface plasmon of an MNS is excited; thus, it seems possible to distinguish between two nearby wavelengths in a small frequency range near $\sim 4.7 \times 10^{15}$ rad/s using a device less than 1 $\mu$m in size. Exciting the surface plasmon in a particular MNS is closely related to the frequencies where the whole system exhibits a large amount of forward or backward scattering of light. This pronounced forward and backward scattering is caused within specific ranges of frequency that allow the collection of MNSs to constructively or destructively add their radiated light. This behavior has exciting experimental consequences such as being able to infer the ohmic power dissipated in an MNS by looking at the scattered light field. Rather than having to coat the MNSs with specific dyes to measure their output power, it should be possible to simply detect the amount of forward and back scattered light. The retardation of the incident and scattered light field removes the symmetry through the middle of the line of nanospheres, allowing a range of complex effects. Only a few of these effects have been discussed in this paper; many variations have not yet been explored and will probably disclose more fascinating effects.

**Acknowledgment.** We would like to gratefully acknowledge fruitful discussions with J. D. Hanson, Albert Polman, and Kobus Kuipers. The work of J.V.H. and F.R. is supported by NSF Grant No. 0098195. Any opinions, findings, and conclusions or recommendations expressed in this material are those of the authors and do not necessarily reflect the views of the National Science Foundation. L.D.N. is part of the research program of the Stichting voor Fundamenteel Onderzoek der Materie (FOM), which is financially supported by the Nederlandse Organisatie voor Wetenschappelijk Onderzoek (NWO).

## References and Notes

(1) Maier, S. A.; Kik, P. G.; Atwater, H. A.; Meltzer, S.; Harel, E.; Koel, B. E.; Requicha, A. A. *Nat. Mater.* **2003**, *2*, 229.
(2) Quinten, M.; Lietner, A.; Krenn, J. R.; Aussenegg, F. R. *Opt. Lett.* **1998**, *23*, 1331.
(3) Krenn, J. R.; et. al. *Phys. Rev. B* **1999**, *82*, 2590.
(4) Müller, J.; et. al. *Appl. Phys. Lett.* **2002**, *81*, 171.
(5) Zentgraf, T.; Christ, A.; Kuhl, J.; Giessen, H. *Phys. Rev. Lett.* **2004**, *93*, 243901.
(6) Brongersma, M. L.; Hartman, J. W.; Atwater, H. A. *Phys. Rev. B* **2000**, *62*, R16356.
(7) Maier, S. A.; Kik, P. G.; Atwater, H. A. *Phys. Rev. B* **2003**, *67*, 205402.
(8) Kelly, K. L.; Coronado, E.; Zhao, L. L.; Schatz, G. C. *J. Phys. Chem. B* **2003**, *107*, 668.
(9) Li, K.; Stockman, M. I.; Bergman, D. *J. Phys. Rev. Lett.* **2003**, *91*, 227402.
(10) Park, S. Y.; Stroud, D. *Phys. Rev. B* **2004**, *69*, 125418.
(11) Citrin, D. S. *Nano Lett.* **2005**, *5*, 985.
(12) Citrin, D. S. *Nano Lett.* **2004**, *4*, 1561.
(13) Colas des Francs, G.; Girard, C.; Martin, O. J. F. *Phys. Rev. Lett* **2003**, *67*, 053805.
(14) Kreibig, U.; Vollmer, M. *Optical Properties of Metal Clusters*; Springer-Verlag: Berlin, 1994.
(15) Jackson, J. D. *Classical Electrodynamics*, 3rd ed.; John Wiley & Sons: New York, 1999.
(16) We will use an index of refraction $n = 1.5$ (the general phenomena in this paper do not depend on $n$).
(17) Johnson, P. B.; Christy, R. W. *Phys. Rev. B* **1972**, *6*, 4370.